



**HAL**  
open science

## Chitosan ascorbate hydrogel improves water uptake capacity and cell adhesion of electrospun poly(epsilon-caprolactone) membranes

Robin Augustine, Pan Dan, Inbar Schlachet, Didier Rouxel, Patrick Menu, Alejandro Sosnik

### ► To cite this version:

Robin Augustine, Pan Dan, Inbar Schlachet, Didier Rouxel, Patrick Menu, et al.. Chitosan ascorbate hydrogel improves water uptake capacity and cell adhesion of electrospun poly(epsilon-caprolactone) membranes. *International Journal of Pharmaceutics*, 2019, 559, pp.420-426. 10.1016/j.ijpharm.2019.01.063 . hal-02276608

HAL Id: hal-02276608

<https://hal.science/hal-02276608v1>

Submitted on 22 Oct 2021

**HAL** is a multi-disciplinary open access archive for the deposit and dissemination of scientific research documents, whether they are published or not. The documents may come from teaching and research institutions in France or abroad, or from public or private research centers.

L'archive ouverte pluridisciplinaire **HAL**, est destinée au dépôt et à la diffusion de documents scientifiques de niveau recherche, publiés ou non, émanant des établissements d'enseignement et de recherche français ou étrangers, des laboratoires publics ou privés.



Distributed under a Creative Commons Attribution - NonCommercial 4.0 International License

## **Chitosan ascorbate hydrogel improves water uptake capacity and cell adhesion of electrospun poly(epsilon-caprolactone) membranes**

Robin Augustine<sup>1,2,\*</sup>, Pan Dan<sup>2</sup>, Inbar Schlachet<sup>1</sup>, Didier Rouxel<sup>3</sup>, Patrick Menu<sup>2</sup>, Alejandro Sosnik<sup>1,\*</sup>

<sup>1</sup> Laboratory of Pharmaceutical Nanomaterials Science, Department of Materials Science and Engineering, Technion-Israel Institute of Technology, De-Jur Building, Technion City, 3200003 Haifa, Israel

<sup>2</sup> Ingénierie Moléculaire et Physiopathologie Articulaire, UMR 7365 CNRS - Université de Lorraine, Vandoeuvre-lès Nancy, F54500, France

<sup>3</sup> Institut Jean Lamour, UMR 7198 CNRS - Université de Lorraine, 54500 Vandoeuvre-lès-Nancy, France

Corresponding authors: RA: [robin@robinlab.in](mailto:robin@robinlab.in)  
AS: [sosnik@technion.ac.il](mailto:sosnik@technion.ac.il)

### **Abstract**

The most important prerequisites for wound coverage matrices are biocompatibility, adequate porosity, degradability and exudate uptake capacity. A moderate hydrophilicity and exudate uptake capacity can often favour cell adhesion and wound healing potential, however, most of the synthetic polymers like polycaprolactone (PCL) are hydrophobic. Hydrogels based on natural polymers can improve the hydrophilicity and exudate uptake capacity of synthetic dressings and improve healing. In this work, we report the development of chitosan ascorbate-infiltrated electrospun PCL membranes. Our study demonstrated that chitosan ascorbate infiltration improves the hydrophilicity as well as water uptake capacity of the membranes and highly favoured the adhesion of human umbilical vein endothelial cells and human mesenchymal stem cells on the membranes.

## Introduction

Impaired wound healing is a medical condition leading to non-healing chronic wounds and foot ulcers resulting in discomfort, increased health care costs and poor quality of life (Guo and Dipietro, 2010). The primary goal of a wound dressing is to prevent the access of pathogens to the wound bed and to maintain appropriate temperature and moisture to facilitate wound healing (Boateng et al., 2008). Excess build-up of exudates in the wound bed is a leading cause of infection and pathogenesis. Wound dressings with good exudate uptake capacity helps to maintain a moist environment and promotes healing. The use of polymeric membranes that facilitate cell adhesion, migration and proliferation can further enhance the healing rate and improve the quality of the regenerated tissue (Augustine et al., 2014).

Synthetic biodegradable polymers are robust biomaterials for wound healing applications due to the ability to tailor their bioactivity, mechanical properties and biodegradability (Lutolf and Hubbell, 2005). However, their capability to support cell adhesion under *in vitro* conditions is not always high (Gautam et al., 2013). Strategies such as functionalization with oligopeptides (e.g., arginyl glycyl aspartic acid, RGD), blending with natural proteins that contain this sequence (e.g., collagen) and interact with cellular integrins or incorporation of other agents such as growth factors is often required (Liu et al., 2012). Natural polymers are more favourable for promoting cell adhesion and proliferation (Malafaya et al., 2007), though they display lower and less tuneable stability under physiological conditions than the synthetic counterparts (Kamoun et al., 2017).

For more than two decades, poly(epsilon-caprolactone) (PCL) has drawn a lot of attention in a plethora of biomedical applications (Woodruff and Hutmacher, 2010). PCL displays several advantages including cost-effectiveness, good biocompatibility and mechanical stability and more controlled biodegradability than other polyesters such as poly(lactide) and poly(pactide-co-glycolide) (Choi et al., 2008, Bayati et al., 2017). Previous studies demonstrated the potential of PCL in tissue regeneration including wound repair (Sundaramurthi et al., 2014, Tra Thanh et al., 2018). However, PCL is highly hydrophobic and thus, it shows negligible ability to absorb wound exudates (Hong, 2011). In addition, electrospun PCL dressings lack functional groups that facilitate cell adhesion, which is an important feature when designing matrices for wound healing (Zhang et al., 2005).

Chitosan, a deacetylated derivative of chitin, presents a series of outstanding features including biodegradability, good biocompatibility, antimicrobial activity, non-toxicity and high versatility of chemical modification (Dutta et al., 2009). In addition, chitosan-based

hydrogels are an appealing class of biomaterial to promote cell adhesion (Croisier and Jérôme, 2013) which may be related to its polycationic nature and ability to interact electrostatically with the negatively-charged cell membrane (Nettles et al., 2002). Chitosan based hydrogels have been extensively investigated in wound healing applications (Shamloo et al., 2018, Asfour et al., 2017). However, its use is challenging owing to a relatively high viscosity and limited aqueous solubility at pH >5.5 (Ilyina et al., 2000) and mechanical properties that can challenge dressing removal (Nwe et al., 2009). On the other hand, it represents an attractive component for the supplementation of biomaterials presenting limited cell adhesion.

Chitosan ascorbate (CA) is an organic salt formed by the reaction of chitosan with ascorbic acid in water and it shows a more pH-independent solubility profile, thus providing more flexibility in biomaterial processing and fabrication (Sekar et al., 2018, Rossi et al., 2008, Elbarbary et al., 2015). For example, some studies showed that CA promotes periodontal tissue repair and regeneration owing to the reduced migration of inflammatory cells (Xuan et al., 2010). Hybrid natural/synthetic polymeric biomaterials can overcome the low mechanical properties and limited biological stability of natural biomaterials and the lack of cell adhesion moieties of PCL by capitalizing the advantageous features of each one of the components.

We hypothesized that the supplementation of electrospun PCL membranes with CA incorporated by physical infiltration is a simple, reproducible and cost-effective strategy to improve cell adhesion and proliferation due to the overall reduction of the hydrophobicity. In addition, conferring moderate hydrophilicity to PCL membranes would augment their capacity to absorb exudates which is highly desirable in wound regeneration. In this framework, this work describes the fabrication and characterization of a novel CA-supplemented PCL composite membranes for wound healing applications.

## **Experimental**

**Materials.** PCL with molecular weight 80,000-120,000 and tripolyphosphate (TPP) were purchased from Sigma Aldrich (St. Louis, MO, US). Chitosan (CS, **degree of deacetylation of 94%** and molecular weight of ~50,000 g/mol) was purchased from Glentham Life Sciences (Corsham, UK). Ascorbic acid (AA) was purchased from Fisher Scientific (Loughborough, UK). NaOH was purchased from Merck (NJ, US). Paraformaldehyde, (3-(4,5-dimethylthiazol-2-yl)-2,5-diphenyltetrazolium bromide) (MTT) and 4',6-diamidino-2-phenylindole dihydrochloride (DAPI) were purchased from Sigma-Aldrich (USA). Phalloidin

was purchased from Thermo Fisher Scientific (Paris, France). The Live/Dead assay kit was supplied by Sigma-Aldrich. Dulbecco's Modified Eagle's Medium (DMEM, Lonza, Basel, Switzerland) was used for the culture of human mesenchymal stem cells (hMSCs). Endothelial basic medium (Lonza) was used for human umbilical vein endothelial cell (HUVEC) culture. Media were supplemented with 10% foetal bovine serum (FBS, Lonza), 100 mg ml<sup>-1</sup> fungizone (Fisher), 100 IU ml<sup>-1</sup> penicillin (Sigma-Aldrich) and 200 mM L-glutamine (Sigma-Aldrich) on culture plates. All other reagents/solvents used in this study were from standard manufacturers and of analytical grade quality.

***Synthesis and characterization of chitosan ascorbate.*** For preparing CA, an exact amount of AA to obtain a 1:1 molar ratio with chitosan deacetylated amino groups was dissolved in distilled water under magnetic stirring for 30 min. Afterwards, chitosan was added to obtain a solution of CA under magnetic stirring for 48 h. The product was dialyzed in water, freeze-dried and characterized by Fourier Transform-Infrared Spectroscopy (FTIR), Proton-Nuclear Magnetic Resonance Spectroscopy (<sup>1</sup>H-NMR), powder X-rays diffraction (PXRD) and differential scanning calorimetry (DSC).

FTIR samples were prepared at 25°C on KBr (Merck Chemicals GmbH, Darmstadt, Germany) disks and pressed to transparency. FTIR spectra were recorded in an Equinox 55 spectrometer (Bruker Optics Inc., Ettlingen, Germany) from 4000 to 400 cm<sup>-1</sup> (32–64 scans with a resolution of 4 cm<sup>-1</sup>).

<sup>1</sup>H-NMR spectra of the different products were recorded in a 400-MHz Bruker® Avance III High Resolution spectrometer (Bruker BioSpin GmbH, Rheinstetten, Germany) and Spin Works 4.0 software (University of Manitoba, Winnipeg, MB, Canada) using 5% w/v solutions in D<sub>2</sub>O with the addition of 25 μL acetic acid-D<sub>4</sub>. Chemical shifts are reported in ppm using the signal of D<sub>2</sub>O (4.75 ppm) as internal standard.

PXRD patterns were obtained in an X-Ray Diffractometer MiniFlex, (Rigaku, Tokyo, Japan) under Bragg-Brentano geometry at a scanning rate of 1.25°/min in the range of 0-600 (with intervals of 0.020) on a Perspex slide.

The thermal properties were analyzed in a DSC 2 STARe system equipped with a thermal analyzer with STARe Software V13 (Mettler-Toledo, Schwerzenbach, Switzerland) with an intracooler (Huber TC100) under a dry N<sub>2</sub> atmosphere (flow of 20 mL min<sup>-1</sup>). For this, samples (5–15 mg) were sealed in 40 μL Al-crucible pans (Mettler-Toledo) and subjected to different heating–cooling cycles (10 °C min<sup>-1</sup>). For chitosan and CA, the treatment was as follows: (i) heating from 25 to 100°C (to erase the thermal history), (ii) isothermal heating at 100°C (30 min, to eliminate water traces), (iii) heating from 100 to 300°C, (iv) cooling from

300 to 25°C and (v) heating from 25 °C to 300 °C. For ascorbic acid, the treatment was as follows: (i) heating from 25 to 300°C and (ii) cooling from 300 to 25 °C. For chitosan and CA, the heating from 25 to 300°C is presented.

***Preparation of chitosan ascorbate infiltrated PCL membranes.*** Electrospun PCL membranes were fabricated according to our previous report (Augustine et al., 2015). Briefly, 15% w/v PCL (molecular weight of 80,000-120,000 g/mol) solutions were prepared in acetone. Then, 10 mL of this solution was loaded in a syringe with an 18-gauge needle and electrospun at a distance of 15 cm tip from the collector. An applied DC voltage of 18 kV and a flow rate of 2.5 mL·h<sup>-1</sup> were maintained during the electrospinning process. After the completion of the electrospinning, deposited membranes were carefully removed and used for the fabrication of CA-loaded membranes.

To produce electrospun PCL membranes supplemented with CA, they were immersed in 1 M NaOH for 4 h to introduce surface hydrophilicity. Then, wet membranes were immersed in CA solution for 4 h to infiltrate the solution into the membrane pores and obtain hybrid PCL/CA composites. Four CA concentrations were used, 0.1% (PCL/CA-0.1), 0.5% (PCL/CA-0.5), 1% (PCL/CA-1) and 2% w/v (PCL/CA-2), to assess its effect on water swelling and cell adhesion. The CA matrix in the hybrid membranes was stabilized by ionic crosslinking with TPP (2.5% w/v in water) and formation of a hydrogel infiltrate. Fabricated composite membranes were dialyzed (regenerated cellulose dialysis membranes, nominal MWCO of 3500 g/mol) in ultrapure water for 2 days to remove unreacted reagents.

***Characterization of the membranes.*** Membranes were characterized by High Resolution-Scanning Electron Microscopy (HR-SEM, Ultraplus, Zeiss, Oberkochen, Germany, acceleration voltage 5 kV, samples were coated with gold), X-Ray Diffractometer (XRD, MiniFlex, Rigaku, Tokyo, Japan, 2θ range 0-60°) and FTIR (see above).

Water contact angles on the surface of the samples were measured by a Digital Contact Angle Measurement System equipped with a CCD camera (Phoenix-KGV-5000). PCL and PCL/CA membranes were placed on the stage of the machine. A small water droplet (Milli-Q-water) was carefully placed on the surface of the electrospun membrane by using the software-controlled system. A series of images of the solution droplet were automatically taken. Contact angle was measured from the captured images. All the experiments were carried out at 26°C and about 65% relative humidity. The experiment was repeated for three sets of samples and the contact angle was expressed as mean ± SD (n = 3).

The swelling of the different membranes was measured by tracking the weight increase during incubation in phosphate buffer solution (PBS, pH = 7.4). For this, two-inch diameter disks of PCL and PCL/CA membranes were accurately weighed were placed in PBS (37°C) and at different time points, samples were taken out, carefully wiped with a lint free cloth to remove unabsorbed water and weighed. Then, each sample was freeze-dried and weighed again. Water uptake is expressed as an increase in weight percent according to Equation 1

$$\text{Swelling (\%)} = [(WW - DW)/DW] \times 100 \quad (1)$$

Where WW and DW are the wet and dry weight of the membrane.

Results are expressed as mean  $\pm$  SD of three experiments.

***Cell compatibility and cell adhesion.*** The cell compatibility and adhesion were investigated with HUVECs and hMSCs. For this, fresh human umbilical cords were obtained after full-term births (caesarean section or normal vaginal delivery) with informed consent using the guidelines approved by the University Hospital Centre of Nancy (France). hMSCs and HUVECs were isolated and amplified as previously reported (El Omar et al., 2016). hMSCs on passage 4 and HUVECs on passage 2 were seeded on PCL and PCL/CA membranes at 50,000 cells/cm<sup>2</sup> and cultured with appropriate medium for 24 h. To visualize cell attachment, samples were fixed with 4% paraformaldehyde for 15 min, permeabilized with 0.5% w/v Triton X-100 solution for 15 min and cell cytoskeletons were stained with phalloidin and nuclei were stained with DAPI. Then, the images were taken with a fluorescent microscope (Leica DMI 3000B, Munich, Germany). To assess cell compatibility of hMSCs and HUVECs on the developed membranes, Live/Dead and MTT assays were carried out according to the corresponding to protocols provided by the manufacturers (n = 3). From the fluorescent images of Live-Dead assay results, live and dead cells were counted and the percentage of viable cells was calculated from Equation 2.

$$\text{Viable cells (\%)} = \text{Live cells/Total cells} \times 100 \quad (2)$$

***Statistical analysis.*** The statistical analysis was performed using the un-paired Student's t-test and "One way ANOVA" with Dunnett's post-test performed using Graph- Pad Prism Version 6.04 (San Diego, CA, USA).

## **Results and Discussion**

**Synthesis of CA.** CA was synthesized by the direct reaction of chitosan and ascorbic acid in water (**Figure 1**).

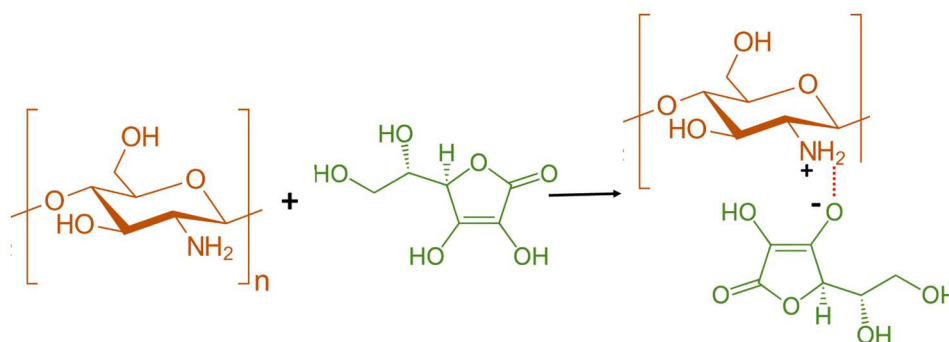


**Figure 1.** Scheme of the formation of CA.

After profuse dialysis to remove any residues and freeze-drying, the formation of the salt was confirmed by FTIR and  $^1\text{H-NMR}$ . FTIR spectra of pure chitosan, ascorbic acid, and CA are shown in **Figure 2A**. Chitosan showed stretching vibration bands of  $-\text{OH}$  and  $-\text{NH}_2$  at  $3465\text{ cm}^{-1}$  (Zhang et al., 2016) and  $-\text{CH}-$  at  $2922$  and  $2845\text{ cm}^{-1}$  (Halevas et al., 2017). Bands at  $1645$  ( $\text{C}=\text{O}$  stretching of amide I) and  $1325\text{ cm}^{-1}$  ( $\text{C}-\text{N}$  stretching of amide III) indicated the presence of residual *N*-acetyl groups due to its partial deacetylation (Ma et al., 2017, Çetinus et al., 2007). Ascorbic acid presents a strong characteristic peak at  $1753\text{ cm}^{-1}$  of  $\text{C}=\text{O}$  stretching of the five-membered lactone ring system and  $1672\text{ cm}^{-1}$  of  $\text{C}=\text{C}$  stretching (Yohannan Panicker et al., 2006). CA shows a shifting and weakening of the band at  $3409\text{ cm}^{-1}$  due to the strong H bonding of  $\text{C}=\text{O}$  of ascorbic acid with amine groups in chitosan and from  $2922$  to  $2846\text{ cm}^{-1}$  with a slight broadening (**Figure 2A**). The characteristic band of ascorbic acid at  $1753\text{ cm}^{-1}$  shifted to  $1720\text{ cm}^{-1}$  in the salt due to the weakening of  $\text{C}=\text{O}$  bond by an inductive effect. In addition, the band at  $1672\text{ cm}^{-1}$  ( $\text{C}=\text{C}$ ) shifted to  $1590\text{ cm}^{-1}$  in CA (**Figure 2A**). Moreover, a new band belonging to ammonium and iminium salt-like structure appeared at  $2354\text{ cm}^{-1}$  (Ragamathunnisa, 2013). In  $^1\text{H-NMR}$ , pure chitosan showed peaks at  $3.0$  ( $\text{H}-\text{C}-\text{NH}_2$ ) and  $3.5$ - $4.0$  ppm (methylene on the backbone) (Xiaolin et al., 2009) and AA at  $4.8$  ( $\text{CH}$ -ring),  $4.02$ - $4.07$  ( $-\text{CH}$ ) and  $3.56$ - $3.67$  ppm ( $-\text{CH}_2$ ) (**Figure 2B**). The carboxylic group of AA reacted with the  $-\text{NH}_2$  of chitosan to form an ammonium carboxylate (**Figure 2**) that results in the shifting of the peak of AA from  $4.8$  to  $4.5$  ppm due to ionic interaction in the formation of a salt (Xiaolin et al., 2009). The  $^1\text{H-NMR}$  spectrum of the salt presented the characteristic peak of primary amine at  $3.00$  ppm, indicating that despite the formation of CA, there were free amine groups for the crosslinking with TPP (**Figure 2B**), as described elsewhere (Rossi et al., 2017). This partial reaction between primary amine moieties and AA most probably stemmed from steric hindrance. In addition, we integrated the relative intensity of this peak at  $3.0$  ppm and compared it to that of pure CS. CA showed a decrease of approximately 23% in the

relative intensity of this peak which indicates the reduction of number of free amine groups compared to CS. These results indicated the successful formation of the salt by the reaction between AA and amine group in CS. In addition, we characterized CA by PXRD and DSC. Both analyses indicated the formation of a completely amorphous salt (**Figure S1**).

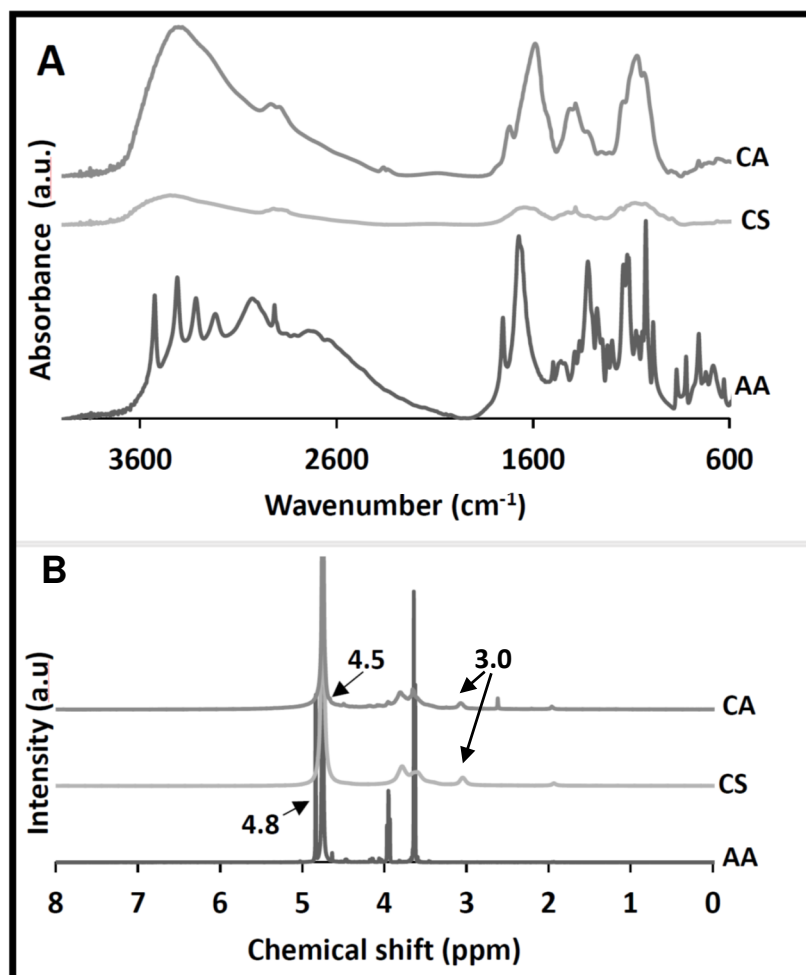


**Figure 2.** (A) FTIR and (B) <sup>1</sup>H-NMR spectra of chitosan (CS), ascorbic acid (AA) and chitosan ascorbate (CA). Peaks at 3 ppm indicate the presence of free amine groups.

**Morphology of PCL/CA membranes.** The morphology of PCL/CA membranes was compared to that of pristine PCL counterparts by HR-SEM. PCL membranes showed the presence of randomly oriented fibers with average diameter of  $1.3 \pm 0.7 \mu\text{m}$  (**Figure 3A**). PCL/CA showed the coating of PCL fibers and the partial filling of the pores with CA (**Figure 3B-D**). The coating slightly modified the fiber diameter and the concentration of CA governed the extent of the coating and membrane infiltration; e.g., PCL/CA-0.5 showed a less efficient infiltration than moderately concentrated solutions. PCL/CA-2 presented

flattened agglomerates of CA on the surface of fibers with an increase of the average diameter to  $4.6 \pm 2.2 \mu\text{m}$  (data not shown). DSC analysis of the composite membranes indicated the presence of CA which was evident from the thermal transitions observed from 150 to 280°C for all the PCL/CA specimens (**Figure S2**). The observed broad peaks might be due to the thermal degradation of CA (Sarasam et al., 2005). Moreover, we observed a 4-9% increase in the dry weight of the membranes after infiltration of CA which confirmed the successful infiltration of CA in the PCL/CA membranes.

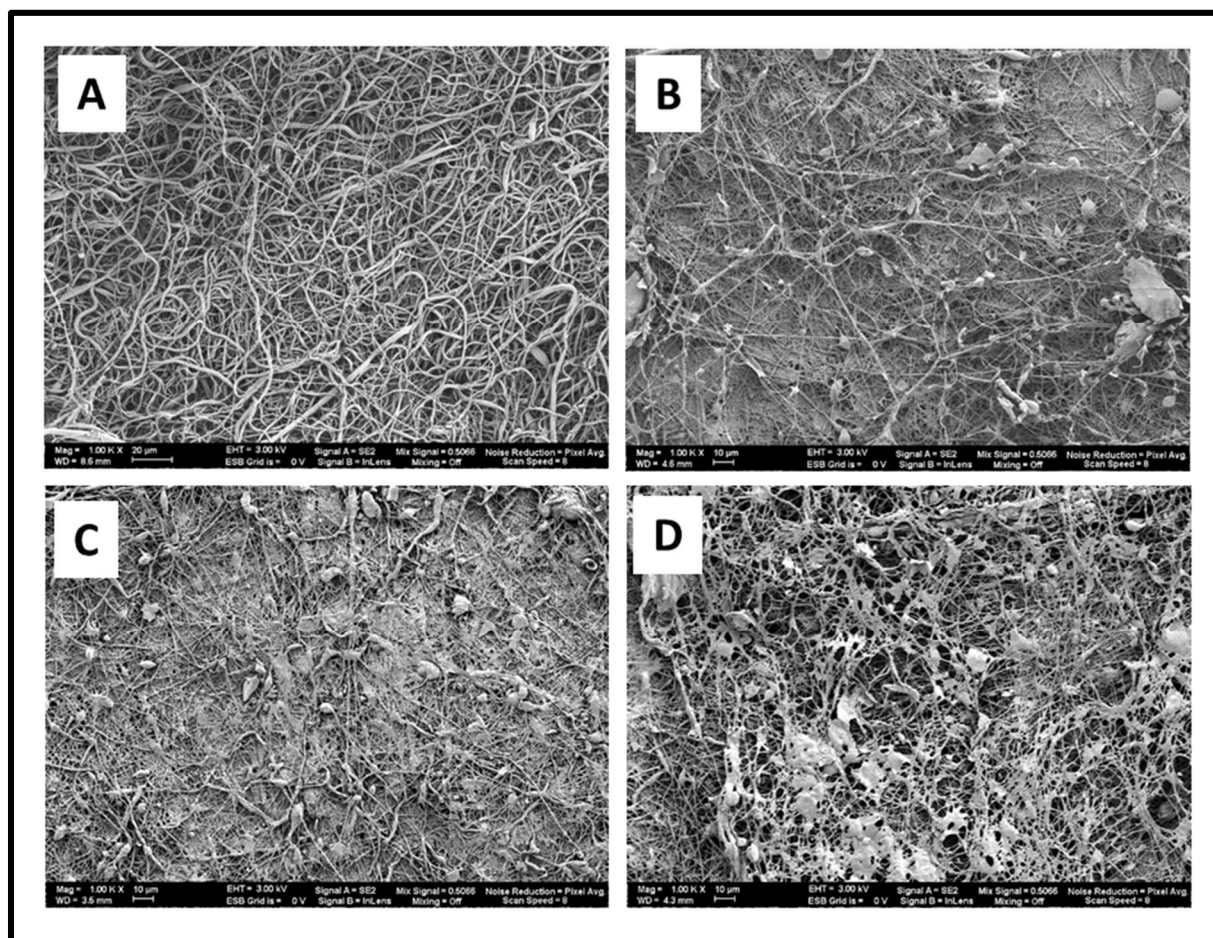


**Figure 3.** High resolution-scanning electron microscopy micrographs of (A) pure PCL, (B) PCL/CA-0.5, (C) PCL/CA-1 and (D) PCL/CA-2 membranes.

**Surface hydrophilicity and swelling.** The surface hydrophobicity can be estimated by measuring the contact angle. Results of water contact angle measurements of pure PCL and PCL/CA membranes obtained by the sessile drop technique are summarized in **Table 1** and exemplified in **Figure S3** for PCL/CA-2. Pure PCL showed a high contact angle of  $104 \pm 6^\circ$  that was consistent with the high hydrophobicity of the surface. NaOH treatment

hydrophilized the surface and the contact angle decrease to  $64 \pm 5^\circ$  owing to a higher wettability, in good agreement with the literature (Wang et al., 2016). The mechanism is the partial hydrolysis of ester bonds of PCL on the fiber surface that increases the concentration of free hydroxyl and carboxyl groups (De Luca et al., 2014). This hydrolysis is not detrimental of the mechanical properties. These groups played a key role to favor the adsorption of CA onto the membrane surface and its retention between inside the pores for the later stabilization by crosslinking. CA modification led to an additional decrease of the contact angle; e.g., PCL/CA-0.5 and PCL/CA-2 showed values of  $53 \pm 5$  to  $47 \pm 8^\circ$  owing to the presence of polar functional groups of chitosan on the surface (Good, 1992). These findings also confirmed the successful modification of the membrane. Similar results were reported for chitosan-coated PCL membranes (Shalumon et al., 2011) and PCL/chitosan blend membranes (Jin et al., 2015).

**Table 1.** Water contact angle measurements on pure PCL and PCL/CA membranes.

Sample	Contact angle (Degrees)
PCL	$104 \pm 6$
NaOH-treated PCL	$64 \pm 5$
PCL/CA-0.5	$53 \pm 5$
PCL/CA-1	$48 \pm 4$
PCL/CA-2	$47 \pm 8$

The capacity to absorb fluids and exudates is a desired property of biomaterials envisioned as wound dressings, particularly of highly-exuding chronic wounds (Mayet et al., 2014). In general, CA supplementation resulted in a substantial increase of the swelling capacity of the membranes (**Figure 4**). PCL membranes did not swell much with values that ranged between  $10.8 \pm 3.5\%$  and  $16.7 \pm 2.8\%$  along the entire assay (6 h). This limited weight gain stemmed from the unspecific retention of aqueous medium inside the small pores of the electrospun hydrophobic membrane. Pretreatment with NaOH increased the hydrophilicity of the membrane surface and thus, the swelling increased to  $80.5 \pm 14.8\%$  to  $127.6 \pm 17.6\%$ . Then, incorporation of CA and its crosslinking, increased the swelling up to approximately 800% owing to the formation of a swollen stable hydrogel (Rossi et al., 2017); as expected, the higher the CA concentration, the more substantial the swelling. These findings are

noteworthy towards the application of these membranes in wound healing and are comparable to those reported for other PCL/chitosan systems (Jin et al., 2015). The application of CA hydrogel infiltrated PCL membranes offers a highly absorbent wound dressing platform that can manage moderate to heavy exudate.

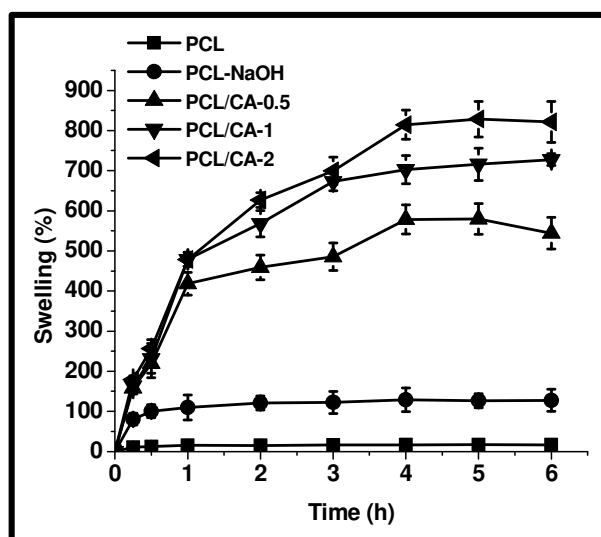


**Figure 4.** Swelling of the different hybrid PCL/CA membranes. Untreated and NaOH-treated (PCL-NaOH) membranes were used as controls.

**Cell adhesion and cell viability studies.** As we described above, we hypothesized that the modification of PCL membranes with CA would improve cell adhesion. To evaluate the cell adhesion properties of these membranes, we seeded hMSCs and HUVECs on the membranes infiltrated with different amounts of CA and compared the results with pure PCL counterparts. In general, cell adhesion and proliferation were higher in all the PCL/CA membranes than in bare PCL membranes with some changes based on the cell type. In the case of hMSCs, PCL/CA-0.5, PCL/CA-1 and PCL/CA-2 showed relatively similar adhesion, indicating that a relatively low amount of CA was sufficient (**Figure 5A, upper row**). However, the difference in hMSC cell adhesion between bare PCL and PCL/CA membranes was marginal. Conversely, in the case of HUVECs, PCL/CA-2 membranes were the most efficient (**Figure 5A, lower row**). The observed differences in cell adhesion behaviour between hMSC and HUVEC on the membranes revealed the intrinsic difference in the inherent nature of the cells. HUVEC are recognized as inactive cells unless stimulated by an extracellular signal such as hypoxia, mechanical stimuli, or biochemical signals (Gupta et al., 2010). In this study, we showed that CA hydrogel coating might have also stimulated the proliferation of HUVEC, the effect being less pronounced for hMSC. Live-dead assay was also carried out to visualize the cells in the membranes (**Figure 5B**). The good cell

compatibility of the membranes and especially of PCL/CA-0.5, PCL/CA-1 and PCL/CA-2 was confirmed by the presence of only few dead cells stained in red by propidium iodide. The percentage of living cells was calculated and presented in **Figure 5C,D**. All the membranes infiltrated with CA showed higher percentage of live cells than pure and NaOH-treated PCL. In addition, the MTT cell metabolic assay confirmed that the membranes are cell compatible with a gradual increase in cell viability for higher CA concentrations (**Figure 5E, F**). These results confirmed the beneficial effect of CA supplementation on the cell compatibility and adhesion *in vitro* of both hMSCs and HUVECs, two cell types that play a fundamental role in wound healing. Future studies will assess the performance of these membranes in murine models of partial wounds.

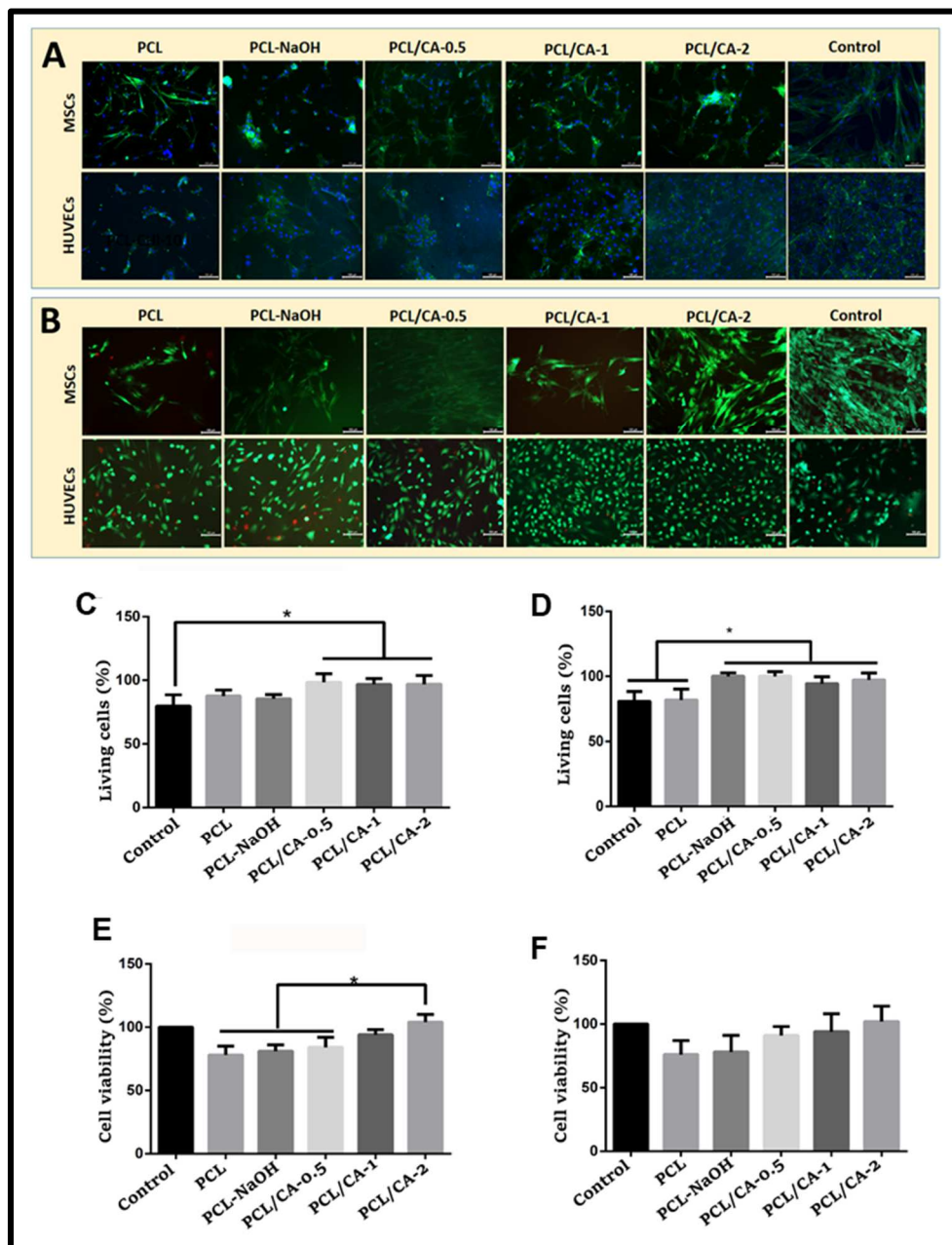


**Figure 5.** Interaction of MSCs and HUVECs with PCL membranes. (A) Fluorescent images of MSCs and HUVECs seeded on PCL, NaOH-treated PCL(PCL-NaOH) and PCL/CA membranes with CA content between 0.5% and 2% w/w, (B) live-dead assay of MSCs and HUVECs cultured on PCL, NaOH-treated PCL and PCL/CA membranes. Green cells are living cells, whereas red coloured cells are dead cells. (C) and (D) are the percentage of living HUVECs and MSCs on the membranes, respectively. (E) and (F) represent the cell viability of HUVECs and MSCs estimated by the MTT assay, respectively.

## Conclusion

In this work, we report on the development and characterization of electrospun PCL membranes infiltrated with different concentrations of CA that result in the formation of a hydrogel filler. HR-SEM analysis confirmed the successful infiltration of CA within the electrospun PCL fibers. Water contact angle and swelling studies demonstrated the increase in hydrophilicity and exudate uptake capacity of the composite membranes. Finally, cell adhesion and compatibility using hMSCs and HUVECs showed better cell adhesion and cell viability on CA hydrogel-supplemented PCL membranes than on pristine counterparts. Owing to the excellent exudate management and cell adhesion properties, the developed PCL/CA membranes are promising for wound healing applications.

## References

- Asfour., M.H., Elmotasem, H., Mostafa, D.M., Salama, A.A., 2017. Chitosan based Pickering emulsion as a promising approach for topical application of rutin in a solubilized form intended for wound healing: In vitro and in vivo study. *Int. J. Pharm.* 534, 325-338.
- Augustine, R., Dominic, E.A., Reju, I., Kaimal, B., Kalarikkal, N., Thomas, S., 2014. Electrospun polycaprolactone membranes incorporated with ZnO nanoparticles as skin substitutes with enhanced fibroblast proliferation and wound healing. *RSC Adv.* 4, 24777-85
- Augustine, R., Dominic, E.A., Reju, I., Kaimal, B., Kalarikkal, N., Thomas, S., 2015. Electrospun poly( $\epsilon$ -caprolactone)-based skin substitutes: In vivo evaluation of wound healing and the mechanism of cell proliferation. *J. Biomed. Mater. Res. - Part B Appl. Biomater.* 103, 1445-1454.
- Bayati, V., Abbaspour, M.R., Dehbashi, F.N., Neisi, N., Hashemitabar, M., 2017. A dermal equivalent developed from adipose-derived stem cells and electrospun polycaprolactone matrix: an in vitro and in vivo study. *Anat. Sci. Int.* 92, 509–20.
- Boateng, J.S., Matthews, K.H., Stevens, H.N.E., Eccleston, G.M., 2008. Wound healing dressings and drug delivery systems: A review. *J Pharm Sci.* 97, 2892-923.
- Çetinus, Ş.A., Öztop, H.N., Saraydin, D., 2007. Immobilization of catalase onto chitosan and cibacron blue F3GA attached chitosan beads. *Enzyme Microb. Technol.* 41, 447-454.
- Choi, J.S., Leong, K.W., Yoo, H.S., 2008. In vivo wound healing of diabetic ulcers using electrospun nanofibers immobilized with human epidermal growth factor (EGF). *Biomaterials* 29, 587–96.
- Croisier, F., Jérôme, C., 2013. Chitosan-based biomaterials for tissue engineering. *Eur. Polym. J.* 49, 780-792.

- De Luca, A.C., Terenghi, G., Downes, S., 2014., Chemical surface modification of poly- $\epsilon$ -caprolactone improves Schwann cell proliferation for peripheral nerve repair. *J. Tissue Eng. Regen. Med.* 8, 153-163.
- Dutta, P.K., Tripathi, S., Mehrotra, G.K., Dutta, J., 2009. Perspectives for chitosan based antimicrobial films in food applications. *Food Chem.* 114, 1173-82.
- El Omar, R., Xiong, Y., Dostert, G., Louis, H., Gentils, M., Menu, P., et al. 2016. Immunomodulation of endothelial differentiated mesenchymal stromal cells: Impact on T and NK cells. *Immunol. Cell. Biol.* 94, 342–356.
- Elbarbary, A.M., Shafik, H.M., Ebeid, N.H., Ayoub, S.M., Othman, S.H., 2015. Iodine-125 Chitosan-Vitamin C Complex: Preparation, characterization and application. *Radiochim. Acta.* 103, 663-71.
- Gautam, S., Dinda, A.K., Mishra, N.C., 2013. Fabrication and characterization of PCL/gelatin composite nanofibrous scaffold for tissue engineering applications by electrospinning method. *Mater. Scie. Eng. C* 33, 1228-35.
- Good, R.J., 1992. Contact angle, wetting, and adhesion: a critical review. *J. Adhes. Sci. Technol.* 6, 1269-1302.
- Guo, S., Dipietro L., 2010. Factors affecting wound healing. *J. Dent. Res.* 89, 219–29.
- Gupta, V., Davis, G., Gordon, A., Altman, A.M., Reece, G.P., Gascoyne, P.R, et al., 2010. Endothelial and stem cell interactions on dielectrophoretically aligned fibrous silk fibroin-chitosan scaffolds. *J. Biomed. Mater. Res. A.* 94, 515-23.
- Halevas, E., Nday, C.M., Chatzigeorgiou, E., Varsamis, V., Eleftheriadou, D., Jackson, G.E, et al., 2017. Chitosan encapsulation of essential oil “cocktails” with well-defined binary Zn(II)-Schiff base species targeting antibacterial medicinal nanotechnology. *J. Inorg. Biochem.* 176, 24–37.
- Hong, S., Kim, G., 2011. Fabrication of electrospun polycaprolactone biocomposites reinforced with chitosan for the proliferation of mesenchymal stem cells. *Carbohydr. Polym.* 83, 940-946.
- Ilyina, A.V., Tikhonov, V.E., Albulov, A.I., Varlamov, V.P., 2000. Enzymic preparation of acid-free-water-soluble chitosan. *Process Biochem.* 35, 563-568.
- Jin, R.M., Sultana, N., Baba, S., Hamdan, S., Ismail, A.F., 2015. Porous pcl/chitosan and nha/pcl/chitosan scaffolds for tissue engineering applications: fabrication and evaluation. *J. Nanomaterials*16, Art. 138.
- Kamoun, E.A, Kenawy, E.R.S., 2017. Chen X. A review on polymeric hydrogel membranes for wound dressing applications: PVA-based hydrogel dressings. *J. Adv. Res.* 3, 217-33.
- Liu, X., Holzwarth, J.M., Ma, P.X., 2012. Functionalized Synthetic Biodegradable Polymer Scaffolds for Tissue Engineering. *Macromol. Biosci.* 12, 911-9.
- Lutolf, M.P., Hubbell, J.A., 2005. Synthetic biomaterials as instructive extracellular microenvironments for morphogenesis in tissue engineering. *Nat. Biotechnol.* 23, 47–55.
- Ma, J., Shi, J., Ding, H., Zhu, G., Fu, K., Fu, X., 2017. Synthesis of cationic polyacrylamide by low-pressure UV initiation for turbidity water flocculation. *Chem. Eng. J.* 312, 20-9.
- Malafaya, P.B., Silva, G.A., Reis, R.L., 2007. Natural–origin polymers as carriers and scaffolds for biomolecules and cell delivery in tissue engineering applications. *Adv. Drug Reliv. Rev.* 59, 207-33.

Mayet, N., Choonara, Y.E., Kumar, P., Tomar, L.K., Tyagi, C., Du Toit, L.C., Pillay, V., 2014. A comprehensive review of advanced biopolymeric wound healing systems. *J. Pharm. Sci.* 103, 2211-2230.

Nettles, D.L., Elder, S.H., Gilbert, J.A., 2002. Potential use of chitosan as a cell scaffold material for cartilage tissue engineering. *Tissue Eng.* 8, 1009-1016.

Nwe, N., Furuike, T., Tamura, H., 2009. The Mechanical and Biological Properties of Chitosan Scaffolds for Tissue Regeneration Templates Are Significantly Enhanced by Chitosan from *Gongronella butleri*. *Materials* 2, 374-398.

Ragamathunnisa M., Jasmine Vasantha Rani E. Padmavathy R., Radha N., 2013. Spectroscopic study on Thiourea and Thiosemicarbazide in Nonaqueous media. *IOSR J. Appl. Phys.* 4, P05-08.

Rossi, S., Marciello, M., Sandri, G., Bonferoni, M.C., Ferrari, F., Caramella, C., 2008. Chitosan Ascorbate : A Chitosan Salt with Improved Penetration Enhancement Properties. *Pharm. Dev. Technol.* 13, 513-21.

Rossi, S., Vigani, B., Puccio, A., Bonferoni, M.C., Sandri, G., Ferrari, F. 2017., Chitosan ascorbate nanoparticles for the vaginal delivery of antibiotic drugs in atrophic vaginitis. *Mar. Drugs* 15, Art. 319.

**Sarasam, A., Madihally, S.V., 2005. Characterization of chitosan–polycaprolactone blends for tissue engineering applications. *Biomaterials*, 26, 5500-8.**

Sekar, V., Rajendran, K., Vallinayagam, S., Deepak, V., Mahadevan, S., 2018. Synthesis and characterization of chitosan ascorbate nanoparticles for therapeutic inhibition for cervical cancer and their in silico modeling. *J. Ind. Eng. Chem.* 62, 239-49.

Shalumon, K.T., Anulekha, K.H., Chennazhi, K.P., Tamura, H., Nair, S.V., Jayakumar, R., 2011. Fabrication of chitosan/poly(caprolactone) nanofibrous scaffold for bone and skin tissue engineering. *Int. J. Biol. Macromol.* 48, 571-576.

Shamloo, A., Sarmadi, M., Aghababaie Z., Vossoughi, M., 2018. Accelerated full-thickness wound healing via sustained bFGF delivery based on a PVA/chitosan/gelatin hydrogel incorporating PCL microspheres. *Int. J. Pharm.* 537, 278-289.

Sundaramurthi, D., Krishnan, U.M., Sethuraman, S., 2014. Electrospun nanofibers as scaffolds for skin tissue engineering. *Polym. Rev.* 54, 348-76.

Tra, T.N., Ho H.M., Tran M.P.N, Do, B.T.T., Nguyen, T.T.H., Thai V.P, et al. 2018. Optimization and characterization of electrospun polycaprolactone coated with gelatin-silver nanoparticles for wound healing application. *Mater. Sci. Eng. C* 91, 318-29.

Wang, W., Caetano, G., Ambler, W.S., Blaker, J.J., Frade, M.A., Mandal, P., et al. 2016. Enhancing the hydrophilicity and cell attachment of 3D printed PCL/graphene scaffolds for bone tissue engineering. *Materials* 9, Art. 992.

Woodruff, M.A., Hutmacher, D.W., 2010. The return of a forgotten polymer-polycaprolactone in the 21st century. *Progr. Polym. Sci.* 35, 1217-56.

Xiaolin, T., Dafeng, T., Zhongyan, W., Fengkui, M., 2009. Synthesis and evaluation of chitosan-vitamin C complexes. *J. Appl. Polym. Sci.* 114, 2986-2991.

Xuan, W., Hong-cheng, J., Yan-min, F., Li-hua, H., 2010. An effectiveness validation: chitosan-ascorbate for periodontal tissue healing and regeneration in a rat periodontitis model. *J. Clin. Rehab. Tissue Eng. Res.* 14, 2268-2272.

Yohannan, P.C., Tresa, V.H., Philip, D., 2006. FT-IR, FT-Raman and SERS spectra of Vitamin C. *Spectrochim. Acta - Part A Mol. Biomol. Spectrosc.* 65, 802-804.

Zhang, S., Xia, L., Ding, C., Wen, L., Wan, W., Chen, G., 2016. Biocompatible nanocarriers that respond to oxidative environments via interactions between chitosan and multiple metal ions. *Int. J. Nanomedicine* 11, Art. 2769.

Zhang, Y.Z., Venugopal, J., Huang, Z. M., Lim, C.T., Ramakrishna, S., 2005. Characterization of the surface biocompatibility of the electrospun PCL-collagen nanofibers using fibroblasts. *Biomacromolecules* 6, 2583-2589.

